ADAPTIVE FUZZY HYBRID MULTICHANNEL FILTERS FOR COLOR IMAGE RESTORATION

Hung-Hsu Tsai and Pao-Ta Yu

Department of Computer Science and Information Engineering
National Chung Cheng University
Chiayi, Taiwan 62107, R.O.C.

ABSTRACT

In this paper, we propose a new class of multichannel filters called adaptive fuzzy hybrid multichannel ($AFHM$) filters to achieve noise attenuation, chromaticity retention, and edges or details preservation simultaneously. Our novel approach mainly based on human concept (heuristic rules) provides a significant framework for taking the merits of filtering behaviors of three filters, a vector median (VM) filter, a vector directional (VD) filter, and an identity filter [1, 2].

1. INTRODUCTION

Recently, vector-processing approach is effectively exploited in the multichannel signal processing due to the consideration of channel dependence. One class of order statistics (OS) multichannel image filters is based on reduced sub-ordering (R-ordering) scheme to obtain order statistics on observed vector-valued samples [3]. Two famous examples, VM and VD filters, have been proposed by [1] and [2], respectively. VM filters are effective in noise attenuation in contrast to the VD filters which are effective in chromaticity retention. Hence, another class of multichannel filters was proposed by combining the characteristics of VM and VD filters, such as distance and directional (DD), and adaptive nearest neighbor multichannel ($ANNM$) filters [4, 5]. However, these filters are difficult to possess the capabilities of noise attenuation, chromaticity retention, and details preservation simultaneously. This motivates us to develop $AFHM$ filters based on fuzzy techniques and learning algorithms such that they can further improve the filtering performance of conventional multichannel filters.

2. BASIC CONCEPTS

2.1. Ranking Vector-Valued Data

A digital multichannel image $\mathcal{I}$ with size $L \times K$ is represented by $\mathcal{I} = [\mathbf{x}_{ij}]_{L\times K}$ where $\mathbf{x}_{ij} \in \{0, 1, 2, \cdots, 255\}^m$. In this paper, $\mathbf{x}_{ij}$ is called the vector-valued pixel located at position $(i,\, j)$ in $\mathcal{I}$. Note that $m = 3$ when the digital multichannel image is an RGB color image. Hereafter, $m = 3$ in this paper, unless otherwise stated. In addition, a filter window with size $N = (2\tau + 1)^2$ (N is odd, in general) covers on the image $\mathcal{I}$ at position $(i,\, j)$ to obtain an observed sample matrix $\mathbf{X}_{ij}$ (or filter window content) defined by $\mathbf{X}_{ij} = \mathbf{X}^{(l)} = \left(\mathbf{x}_1^{(l)},\, \mathbf{x}_2^{(l)},\, \cdots,\, \mathbf{x}_k^{(l)},\, \cdots,\, \mathbf{x}_{N-1}^{(l)},\, \mathbf{x}_N^{(l)}\right)$ where $1 \le i \le L$ and $1 \le j \le K$. In addition, $\mathbf{x}_k^{(l)} = [x_{rk}^{(l)},\, x_{gk}^{(l)},\, x_{bk}^{(l)}]^T,\, x_{rk}^{(l)},\, x_{gk}^{(l)},\, x_{bk}^{(l)} \in \{0,\, 1,\, \cdots,\, 255\}$, $1 \le k \le N$ and T denotes the matrix transpose.

The ordering of $\mathbf{x}_1^{(l)},\, \mathbf{x}_2^{(l)},\, \cdots$, and $\mathbf{x}_N^{(l)}$ based on R-ordering scheme is according to distance criteria or functions. An aggregated distance corresponding to $\mathbf{x}_i^{(l)}$ can be defined by $d_i^{(l)} = \sum_{j=1}^{N} \rho\left(\mathbf{x}_i^{(l)},\, \mathbf{x}_j^{(l)}\right)$ where $\rho : \{0,\, 1,\, \cdots,\, 255\}^3 \times \{0,\, 1,\, \cdots,\, 255\}^3 \to R$ is a distance function. For instance, ρ can be one of Minkowski metrics defined by

$$\rho\left(\mathbf{x}_i^{(l)},\, \mathbf{x}_j^{(l)}\right) = \left[\sum_{k\in\{r,\, g,\, b\}} \left|x_{ki}^{(l)} - x_{kj}^{(l)}\right|^p\right]^{\frac{1}{p}}, \qquad (1)$$

or be the vector angle distance defined by

$$\rho\left(\mathbf{x}_i^{(l)},\, \mathbf{x}_j^{(l)}\right) = \arccos\left(\frac{\mathbf{x}_i^{(l)^T}\mathbf{x}_j^{(l)}}{\left\|\mathbf{x}_i^{(l)}\right\|\left\|\mathbf{x}_j^{(l)}\right\|}\right). \qquad (2)$$

Note that (1) is called Block (L_1 norm), Euclidean (L_2 norm) and Max (L_∞ norm) distances while $p = 1,\, 2$, and ∞, respectively [2, 5]. Thus, each $\mathbf{x}_i^{(l)}$ is reduced

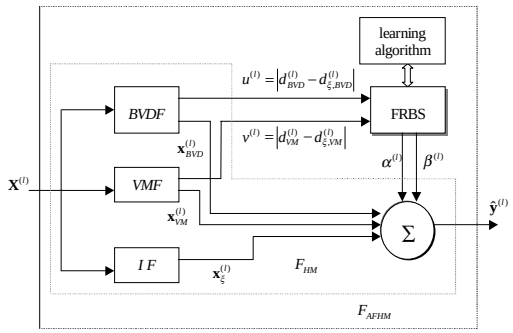

Figure 1: The structure of an $AFHM$ filter.

to a scalar $d_i^{(l)}$ through the mapping of aggregated distances. Let $d_1^{(l)}$, $d_2^{(l)}$,$\cdots$, $d_N^{(l)}$ be sorted in ascending order to become

$$d_{(1)}^{(l)} \leq d_{(2)}^{(l)} \leq \cdots \leq d_{(N)}^{(l)}. \tag{3}$$

On the basis of the total ordering of real numbers, (3) defines a R-ordering of $\mathbf{x}_1^{(l)}$, $\mathbf{x}_2^{(l)}$, $\cdots$, and $\mathbf{x}_N^{(l)}$, that is, $\mathbf{x}_{(1)}^{(l)} \leq \mathbf{x}_{(2)}^{(l)} \leq \cdots \leq \mathbf{x}_{(N)}^{(l)}$.

2.2. Review of VM and VD Filters

First, the design of VM filters is based on the aggregated Euclidean distance to select a minimal entry from the observed sample matrix $\mathbf{X}^{(l)}$ [1]. Let F_{VM} be the window operator associated with a VM filter, which is defined by $\mathbf{x}_{VM}^{(l)} = F_{VM}\left(\mathbf{X}^{(l)}\right) = \mathbf{x}_{(1)}^{(l)}$. Then, the design of VD filters is based on the aggregated vector angle distance. One class of VD filters called basic vector directional (BVD) filters is to select a minimal entry from the observed sample matrix $\mathbf{X}^{(l)}$ [2]. Let F_{BVD} be the window operator associated with a BVD filter, which is defined by $\mathbf{x}_{BVD}^{(l)} = F_{BVD}\left(\mathbf{X}^{(l)}\right) = \mathbf{x}_{(1)}^{(l)}$.

3. THE DESIGN OF $AFHM$ FILTERS

The structure of an $AFHM$ filter is illustrated in Figure 1. The structure of $AFHM$ filters is composed of three principal components: an HM filter, a fuzzy rule-based system (FRBS), and a learning algorithm.

3.1. HM Filters

The structure of an HM filter comprises four basic components: $BVDF$, VMF, IF and a summation combinator. $BVDF$, VMF, and IF stand for a BVD, a VM and an identity filters, respectively. The summation combinator is represented by $\sum$.

Definition 1 *Let F_{HM} be the window operator associated with an HM filter. The output of the HM filter is defined by*

$$F_{HM}\left(\mathbf{X}^{(l)}; \alpha^{(l)}, \beta^{(l)}\right) = \widehat{\mathbf{y}}^{(l)} = \left(1-\alpha^{(l)}\right)\beta^{(l)} \mathbf{x}_{BVD}^{(l)} + \left(1-\beta^{(l)}\right)\mathbf{x}_{VM}^{(l)} + \alpha^{(l)}\beta^{(l)}\mathbf{x}_{\xi}^{(l)} \tag{4}$$

where $\alpha^{(l)}$, $\beta^{(l)} \in [0, 1]$. $\mathbf{x}_{\xi}^{(l)}$ denotes the central vector-valued pixel of a filter window when the filter window covers on an image at position (l) (i.e., at (i, j)). $\mathbf{x}_{BVD}^{(l)}$, $\mathbf{x}_{VM}^{(l)}$, and $\mathbf{x}_{\xi}^{(l)}$ are the outputs of a BVD, a VM, and an identity filters, respectively. The output of the HM filter is denoted as $\widehat{\mathbf{y}}^{(l)} = \left[\widehat{y}_r^{(l)}, \widehat{y}_g^{(l)}, \widehat{y}_b^{(l)}\right]^T$, and $\widehat{y}_r^{(l)}, \widehat{y}_g^{(l)}, \widehat{y}_b^{(l)} \in \{0, 1, \cdots, 255\}$. □

Two control values, $\alpha^{(l)}$ and $\beta^{(l)}$, decide the coefficients within (4) to adapt the window content $\mathbf{X}^{(l)}$. The HM filter is called the $AFHM$ filter when $\alpha^{(l)}$ and $\beta^{(l)}$ are decided by fuzzy techniques and learning algorithms. In this paper, one of the main contributions is to apply an FRBS and a gradient-descent learning algorithm for adjusting these two control values such that the $AFHM$ filters can adapt the distinct window contents. Before we state the design of the FRBS and the learning algorithm to decide $\alpha^{(l)}$ and $\beta^{(l)}$, we give some deterministic properties of HM filters for deeply understanding the behavior of HM filters.

Property 1: HM filters are invariant under scaling.

Property 2: HM filters are invariant under rotation when ρ is the L_2 norm on the design of VM filters.

Property 3: Suppose that $\alpha^{(l)} \neq 1$ and $\beta^{(l)} \neq 1$. An input image $\mathcal{I}$ is a root of the HM filter of length N if and only if the central vector-valued pixel of the window $\mathbf{x}_{\xi}^{(l)}$ is a convex combination of $\mathbf{x}_{BVD}^{(l)}$ and $\mathbf{x}_{VM}^{(l)}$, that is, $\mathbf{x}_{\xi}^{(l)} = \lambda\mathbf{x}_{BVD}^{(l)} + (1-\lambda)\mathbf{x}_{VM}^{(l)}$ where $\lambda = \frac{\left(1-\alpha^{(l)}\right)\beta^{(l)}}{1-\alpha^{(l)}\beta^{(l)}}$.

3.2. The Design Motivation of $AFHM$ Filters

According to human concept, four cases are considered on the design of $AFHM$ filters. Let $d_{VM}^{(l)}$ and $d_{BVD}^{(l)}$ denote the aggregated distances corresponding to $\mathbf{x}_{VM}^{(l)}$ and $\mathbf{x}_{BVD}^{(l)}$, respectively. In addition, let $d_{\xi,VM}^{(l)}$ and $d_{\xi,BVD}^{(l)}$ denote the aggregated distances corresponding to $\mathbf{x}_{\xi}^{(l)}$ based on ρ defined by (1) and (2), respectively. Then, we define $u^{(l)} = \left|d_{VM}^{(l)} - d_{\xi,VM}^{(l)}\right|$ and $v^{(l)} = \left|d_{BVD}^{(l)} - d_{\xi,BVD}^{(l)}\right|$.

In the first case, when $u^{(l)}$ is large and $v^{(l)}$ is large, this indicates that the possibility of that $\mathbf{x}_\xi^{(l)}$ is corrupted should be very high. The behavior of the $AFHM$ filter is emphasized to inherit the noise-attenuation and chromaticity-retention capabilities from the VM and the BVD filters, respectively. Therefore, from Figure 1, this kind of behavior can be decided by $\alpha^{(l)}$ and $\beta^{(l)}$, in (4). That is, $\alpha^{(l)}$ and $\beta^{(l)}$ should be low to result in that the coefficient associated with $\mathbf{x}_\xi^{(l)}$ approaches to zero.

In the second case, when $u^{(l)}$ is small and $v^{(l)}$ is large, this indicates that $\mathbf{x}_\xi^{(l)}$ is regarded as an uncorrupt vector by the VM filter, whereas $\mathbf{x}_\xi^{(l)}$ is regarded as a corrupted vector by the BVD filter. This occurs a conflict whether $\mathbf{x}_\xi^{(l)}$ is corrupted or not. In this case, for the sake of details preservation, the possibility of contributing $\mathbf{x}_{BVD}^{(l)}$ to the output of the $AFHM$ should be low. Therefore, the behavior of the $AFHM$ filter is emphasized to inherit the noise-attenuation and details-preservation capabilities from the VM and the identity filters, respectively. Consequently, in (1), $\alpha^{(l)}$ should be high and $\beta^{(l)}$ should be low to result in that the coefficient associated with $\mathbf{x}_{BVD}^{(l)}$ approaches to zero.

In the third case, when $u^{(l)}$ is large and $v^{(l)}$ is small, this indicates that $\mathbf{x}_\xi^{(l)}$ is regarded as a corrupted vector by the VM filter, whereas $\mathbf{x}_\xi^{(l)}$ is regarded as an uncorrupted vector by the BVD filter. This also occurs a conflict which is a converse case with respect to the second case. For the sake of details preservation, the possibility of contributing $\mathbf{x}_{VM}^{(l)}$ to the output of the $AFHM$ should be low. The behavior of the $AFHM$ filter is emphasized to inherit the chromaticity-retention and details-preservation capabilities of the BVD and the identity filters, respectively. Consequently, in (1), $\alpha^{(l)}$ should be low and $\beta^{(l)}$ should be high to result in that the coefficient associated with $\mathbf{x}_{VM}^{(l)}$ approaches to zero.

In the fourth case, when $u^{(l)}$ is small and $v^{(l)}$ is small, this indicates that the possibility of that two median vectors outputted by the VM and the BVD filters are $\mathbf{x}_\xi^{(l)}$ should be very high. For the reason of details preservation, the possibility of reducing the output of the $AFHM$ filter to be $\mathbf{x}_\xi^{(l)}$ should be very high. In this case, the output of the $AFHM$ filter achieves three objectives simultaneously. So, in (1), $\alpha^{(l)}$ and $\beta^{(l)}$ should be very high to result in that the coefficients associated with $\mathbf{x}_{VM}^{(l)}$ and $\mathbf{x}_{BVD}^{(l)}$ approach to zero.

From above scenario, the behavior of the $AFHM$ filter is heavily controlled by $\alpha^{(l)}$ and $\beta^{(l)}$. The functions of $\alpha^{(l)}$ and $\beta^{(l)}$, however, are highly nonlinear and are difficult to be precisely represented by convectional mathematical models. In this paper, we propose an FRBS and a learning algorithm to adjust $\alpha^{(l)}$ and $\beta^{(l)}$ such that $AFHM$ filters are capable of taking the merits of the behavior of a VM, a BVD, and an identity filters for achieving these three objectives.

3.3. The Design of the FRBS

An FRBS consists of a set of fuzzy rules represented in IF-then format [6]. According to human concept stated in Subsection 3.2, the behavior of the $AFHM$ filter can be described by means of four fuzzy rules:

R1: If $u^{(l)}$ is *large* and $v^{(l)}$ is *large*, then $\alpha^{(l)}$ is *low* and $\beta^{(l)}$ is *low*

R2: If $u^{(l)}$ is *small* and $v^{(l)}$ is *large*, then $\alpha^{(l)}$ is *high* and $\beta^{(l)}$ is *low*

R3: If $u^{(l)}$ is *large* and $v^{(l)}$ is *small*, then $\alpha^{(l)}$ is *low* and $\beta^{(l)}$ is *high*

R4: If $u^{(l)}$ is *small* and $v^{(l)}$ is *small*, $\alpha^{(l)}$ is *very high* and $\beta^{(l)}$ is *very high*.

where, $u^{(l)}$ and $v^{(l)}$ are two linguistic variables, and five linguistic terms, *small*, *large*, *high*, *low*, *very high* can be expressed by fuzzy sets with 1-D shape membership functions such as bell-shape 1-D functions. Consequently, two 2-D continuous functions, for instance, in Figure 2, to decide $\alpha^{(l)}$ and $\beta^{(l)}$ can be obtained if these four fuzzy rules are merged [7]. These two 2-D functions can be viewed as the membership functions of $\alpha^{(l)}$ and $\beta^{(l)}$. In most fuzzy rule-based systems with fuzzy inference techniques, these two 2-D membership functions are obtained by merging 1-D membership functions of linguistic terms, *small* and *large*, and their fuzzy relations to $\alpha^{(l)}$ and $\beta^{(l)}$ [6]. However, in some applications such as the field of signal processing, it is difficult to obtain these two membership functions accurately. The problem can be circumvented via using approximated functions which can be obtained by a learning approach [7].

3.4. Learning Algorithm

The 1-D nonlinear continuous membership function can be approximated by a 1-D step-shape function. Hence, the 2-D continuous membership functions can be approximated by 2-D step-shape functions which comprises a finite number of piecewise regions, such as Figure 3(a) and (b). These two 2-D step-shape functions are the membership functions to characterize $\alpha^{(l)}$ and $\beta^{(l)}$, respectively. Let the heights of region (p, q) in these two 2-D step-shape functions be $\alpha_{p,q}$ and $\beta_{p,q}$, respectively. Therefore, the values of $\alpha_{p,q}$ and $\beta_{p,q}$ can be trained by the least mean squared (LMS) algorithm which is subject to minimize the cost function (or error

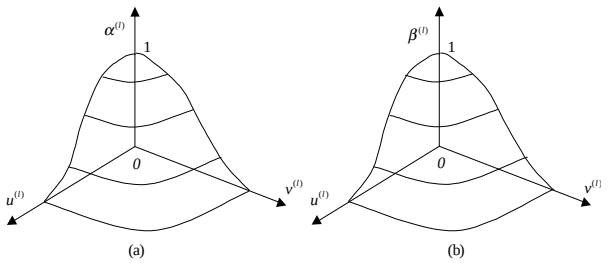

Figure 2: (a) an example of the shape of linguistic variable $\alpha^{(l)}$; (b) an example of the shape of linguistic variable $\beta^{(l)}$.

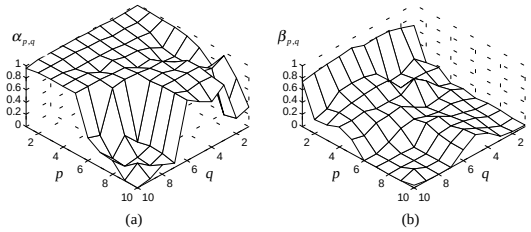

Figure 3: (a) and (b) are two 2-D step-shape membership functions to characterize linguistic variables $\alpha^{(l)}$ and $\beta^{(l)}$, respectively.

surface) $\varepsilon_{p,q}$ with respect to region (p,q) [9]:

$$\varepsilon_{p,q} = \frac{1}{2}E\left[\|\mathbf{e}\|^2\right] = \frac{1}{2}E\left[\left\|\mathbf{y}^{(l)} - \widehat{\mathbf{y}}^{(l)}\right\|^2\right] \qquad (5)$$

where $\mathbf{e}$ represents the estimated-error vector, $\forall l \in S_{p,q} = \left\{j : \left(h_1\left(u^{(j)}\right), h_2\left(v^{(j)}\right)\right) = (p,q)\right\}$, and E denotes the statistical expectation operator. Moreover, $\mathbf{y}^{(l)}$ is the desired pixel and $\widehat{\mathbf{y}}^{(l)}$ is the output pixel of the $AFHM$ filter. Let $1 \le n \le |S_{p,q}|$ where $|S_{p,q}|$ denotes the cardinality of the index set $S_{p,q}$. In (5), $\alpha_{p,q}$ and $\beta_{p,q}$ constitute the error surface $\varepsilon_{p,q}$. On the basis of the gradient-decent method, $\alpha_{p,q}$ and $\beta_{p,q}$ can be adjusted in an iterative fashion along with the error surface toward the optimum solution. Then, the updated rules of $\alpha_{p,q}$ and $\beta_{p,q}$ can be, respectively, obtained as:

$$\begin{aligned}\alpha_{p,q}(n+1) &= \alpha_{p,q}(n) + \eta_{p,q}(n) \\ &\beta_{p,q}(n)\left(\mathbf{y}^{(l)} - \widehat{\mathbf{y}}^{(l)}\right)^T\left(\mathbf{x}_{\xi}^{(l)} - \mathbf{x}_{BVD}^{(l)}\right)\end{aligned} \qquad (6)$$

and

$$\begin{aligned}\beta_{p,q}(n+1) &= \beta_{p,q}(n) + \eta_{p,q}(n)\left(\mathbf{y}^{(l)} - \widehat{\mathbf{y}}^{(l)}\right) \\ &\left[\mathbf{x}_{BVD}^{(l)} - \mathbf{x}_{VM}^{(l)} + \alpha_{p,q}(n)\left(\mathbf{x}_{\xi}^{(l)} - \mathbf{x}_{BVD}^{(l)}\right)\right]\end{aligned} \qquad (7)$$

where $\eta_{p,q}$ denotes the learning-rate parameter associated with region (p,q) [9]. Consequently, the function values of all piecewise regions can be obtained via the training process. For instance, the two membership functions of linguistic variables $\alpha^{(l)}$ and $\beta^{(l)}$ represented by 2-D step-shape functions are depicted in Figure 3(a) and (b), respectively. For example, $p = 4$ denotes $0.3 \le u^{(l)} < 0.4$, and $q = 6$ denotes $0.5 \le v^{(l)} < 0.6$. Hence, $\alpha^{(l)}$ is $\alpha_{4,6} = 0.978$ and $\beta^{(l)}$ is $\beta_{4,6} = 0.295$. Finally, we investigate the convergence property of the learning algorithm mentioned above.

Property 4: Let the lth training pattern $(\mathbf{X}^{(l)}, \mathbf{y}^{(l)})$ belong to region (p,q), and l be the nth element of $S_{p,q}$. That is, on the basis of pattern-by-pattern fashion $(\mathbf{X}^{(l)}, \mathbf{y}^{(l)})$ is regarded as the nth training pattern associated with region (p,q). According to updated rules (6) and (7), the learning algorithm converges with respect to region (p,q) if $\eta_{p,q}(n)$ is chosen as

$$\begin{aligned}\eta_{p,q}(n) = \eta_0 / \Bigg(&\left\|\mathbf{x}_{BVD}^{(l)} - \mathbf{x}_{VM}^{(l)}\right\|^2 + \\ &\left[\alpha_{p,q}^2(n) + \beta_{p,q}^2(n)\right]\left\|\mathbf{x}_{\xi}^{(l)} - \mathbf{x}_{BVD}^{(l)}\right\|^2\Bigg)\end{aligned} \qquad (8)$$

where η_0 is the initial value of learning-rate parameter, and $0 < \eta_0 \le 1$. Note that using the similar way we can prove that this learning algorithm converges with respect to other regions.

4. SIMULATION RESULTS

In this simulation, a number of RGB color images with size 480×512 are examined, which include Tree, Peppers, Lenna and Baboon images. The artificial additive noises are generated in the corrupted process. In addition, a kind of channel dependence is simulated by correlation coefficients ρ_{RG}, ρ_{GB}, and ρ_{BR} which are 0.5 in this simulation. Two measures are used to assess the filtering performance. The first measure is the normalized mean squared error (NMSE) which is a standard quantitative measure: NMSE $= \frac{\sum_{l=1}^{L\times K}\left\|\mathbf{y}^{(l)} - \widehat{\mathbf{y}}^{(l)}\right\|^2}{\sum_{l=1}^{L\times K}\left\|\mathbf{y}^{(l)}\right\|^2}$ where $\mathbf{y}^{(l)}$ and $\widehat{\mathbf{y}}^{(l)}$ represent the original and the estimated image vector-valued pixels, respectively. Another measure is the mean color difference (MCD) which is based on the $L^*a^*b^*$ space: MCD $= \frac{\sum_{l=1}^{L\times K}\left\|\mathbf{h}^{(l)} - \widehat{\mathbf{h}}^{(l)}\right\|^2}{L\times K}$ where $\mathbf{h}^{(l)}$ and $\widehat{\mathbf{h}}^{(l)}$ are the points in the $L^*a^*b^*$ space corresponding to $\mathbf{y}^{(l)}$ and $\widehat{\mathbf{y}}^{(l)}$, respectively [2, 5]. MCD indicates the error of color images in human perception. The comparisons

of filtered results are shown in Tables 1 and 2. Let $AFHM_{\mathrm{B}}$, $AFHM_{\mathrm{T}}$, $AFHM_{\mathrm{P}}$ and $AFHM_{\mathrm{L}}$ represent an $AFHM$ filter individually trained by Baboon, Tree, Peppers, and Lenna images in advance, respectively. Obviously, the filtering performance of $AFHM$ filters is better than that of other simulated filters under consideration. One of methods for assessing details preserving is to compare the filtering results of the noise-free (0%) original images. To observe Tables 1 and 2, the details-preserving capability of $AFHM$ filters is superior to that of simulated filters under consideration. In order to assess the robust capability the training and testing images should be different [7, 9]. In this simulation, the training images include Tree, Peppers and Lenna images with the same probability of impulsive noises as Baboon image. Table 3 illustrates that $AFHM$ filters also possess the robust capability.

5. CONCLUSIONS

A novel class of nonlinear multichannel filters called $AFHM$ filters has been proposed in this paper. On the design of $AFHM$ filters, human concept has been efficiently expressed by fuzzy rules to decide control values. Moreover, a faster learning algorithm based on the LMS algorithm are employed to improve the filtering performance and to enhance the robust capability of $AFHM$ filters. Finally, the simulation results illustrate that $AFHM$ filters possess not only the capabilities of noise attenuation, chromaticity retention, and edges or details preservation but also the capabilities of the robustness and adaptation.

6. REFERENCES

[1] J. Astola, P. Haavisto and Y. Neuvo, "Vector median filtering," *IEEE Proc.*, vol. 78, no. 4, pp. 678-689, Apr. 1990.

[2] P. E. Trahanias, D. Karakos and A. N. Venetsanopoulos, "Directional processing of color images: theory and experimental results," *IEEE Trans. Image Processing*, vol. 5, no. 6, pp. 868-880, Jun. 1996.

[3] V. Barnett, "The ordering of multivariate data," *J. Royal Stat. Soc. A,* vol. 139, part 3, pp. 318-343, 1976.

[4] D. Karakos and P. E. Trahanias, "Generalized multichannel image-filtering structures," *IEEE Tran. Image processing*, vol. 6, no. 7, pp. 1038-1045, Jul. 1997.

filters	0%	4%	6%	10%
VM	2.96	3.12	3.34	3.70
BVD	5.44	5.44	5.65	6.05
DD	2.97	3.07	3.26	3.56
$ANNM$	2.78	2.85	3.07	3.38
$AFHM_{\mathrm{B}}$	0.02	0.85	1.92	2.45

Table 1: NMSE ($\times 10^{-2}$) result for for Baboon image corrupted by impulsive noises.

filters	0%	4%	6%	10%
VM	25.47	27.19	29.16	31.66
BVD	24.91	25.13	26.23	27.78
DD	24.50	25.08	26.70	28.69
$ANNM$	23.61	24.56	27.26	30.33
$AFHM_{\mathrm{B}}$	0.91	8.47	20.72	25.54

Table 2: MCD result for Baboon image corrupted by impulsive noises.

[5] K. N. Plataniotis, V. Sri, D. Androutsos and A. N. Venetsanopoulos, "An adaptive nearest neighbor multichannel filters," *IEEE Trans. Circuits and Systems for Video Technology*, vol. 6, No. 6, pp. 699-703, Dec. 1996.

[6] G. J. Klir, B. Yuan, *Fuzzy Sets and Fuzzy Logic Theory and Applications.* Upper Saddle River, NJ: Prentice-Hall, 1995.

[7] K. Arakawa, "Median filters based on fuzzy rules and its application to image processing," *Fuzzy Sets and Systems*, vol. 77, pp. 3-13, 1996.

[8] K. Tang, J. Astola, and Y. Neuvo, "Nonlinear multivariate images filtering techniques," *IEEE Trans. Image Processing*, vol. 4, no. 6, pp. 788-798, Jun. 1995.

[9] S. Haykin, *Neural networks.* New York: Macmillan College Publishing Company, 1995.

	Baboon (6%)		
	$AFHM_{\mathrm{T}}$	$AFHM_{\mathrm{L}}$	$AFHM_{\mathrm{P}}$
NMSE	2.639	2.645	2.721
MCD	20.23	21.03	20.89

Table 3: Filtered results to robust capability for $AFHM$ filters.